

SUPPLEMENTARY INFORMATION

Synthesis and characterization of novel 7-oxy-3-ethyl-6-hexyl-4-methylcoumarin substituted metallo phthalocyanines and investigation of their photophysical and photochemical properties.

Mücahit Özdemir,^a Begümhan Karapınar,^a Bahattin Yalçın,^{*a} Ümit Salan,^a Mahmut Durmuş^b and Mustafa Bulut^{*a}

a. Marmara University, Department of Chemistry, 34722 Kadikoy, Istanbul, Turkey. E-mail: byalcin@marmara.edu.tr, mbulut@marmara.edu.tr, mozdemir17@marun.edu.tr, usalan@marmara.edu.tr, begumhankarapinar@gmail.com

b. Gebze Technical University, Department of Chemistry, 41400 Gebze, Kocaeli, Turkey. E-mail: durmus@gtu.edu.tr

1. Experimental

1.1. Materials

All chemicals used were of reagent grade quality. 3-Nitrophthalonitrile, 4-nitrophthalonitrile, 4,5-dichlorophthalonitrile, 7-hydroxy-3-ethyl-6-hexyl-4-methylcoumarin (**1**) and its phthalonitrile derivatives (**2-5**) were synthesized and purified according to the methods described previously in literature respectively.¹⁻³ 4-Hexylresorcinol, ethyl 2-ethylacetoacetate, 1,3-diphenylisobenzofuran (DPBF) and metal salts were purchased from Sigma-Aldrich and used as received. The solvents were purified, dried and stored over 4 Å molecular sieves. All reactions were carried out under high purity N₂ atmosphere unless otherwise noted. The Pc compounds (**6a-9b**) were purified successively by washing with hot acetic acid, water, ethanol and acetonitrile in the Soxhlet apparatus. Column chromatography was performed on silica gel 60 (0.040-0.063 mm) for a proper purification. Melting points of the Pc compounds were found to be higher than 300°C. The homogeneity of the products was tested in each step by thin layer chromatography (TLC Silica gel 60 F₂₅₄).

1.2. Equipment

IR spectra were recorded on a Perkin Elmer Spectrum One fourier transform infrared spectrophotometer. ¹H-NMR spectras were recorded on a Bruker Avance III 500 MHz Three channel NMR spectrometer. Elemental analyses were performed by the Instrumental Analysis Laboratory of the TUBITAK, Marmara Research Centre. Mass spectra were recorded on the Bruker microflex LT MALDI-TOF Mass Spectrometer equipped with a nitrogen UV-Laser operating at 337 nm using the 2,5-dihydroxybenzoic acid (DHB) and dithranol (DIT) matrix. Optical spectra in the UV-vis region were recorded with a Shimadzu 2450 UV-vis spectrophotometer. Fluorescence lifetimes were measured using a time correlated single photon counting setup (TCSPC) (Horiba Fluorolog 3 equipment.) Fluorescence excitation and emission spectra were recorded on the Hitachi F-7000 spectrofluorometer using 1 cm path length cuvette at room temperature. Photo-irradiations were done using a Osram optic halogen lamp (300W-120V). A 600 nm glass cut off filter (Schott) and a water filter were used to filter off ultraviolet and infrared radiations respectively. An interference filter (Intor, 670 nm and 700 nm with a band width of 40 nm) was additionally placed in the light path before the sample. Light intensities were measured with a POWER MAX PM5100 laser (Molelectron detector incorporated) power meter. Thermal properties of phthalocyanines were examined by Thermal Gravimetric Analysis (TGA) using a Perkin-Elmer Thermogravimetric analyzer STA6000 model. TGA curves of the phthalocyanines were obtained in the 30-750°C temperature range with heating rate of 10°C/min under air and N₂ atmospheres. Phase change properties and phase transitions of phthalocyanines were examined by Pyris Diamond differential scanning calorimeter (DSC). DSC analysis was run from 0°C to 80 with 5°C/min heating and cooling rates under N₂ at 25 ml/min.

1.3. Photophysical Parameters

1.3.1. Fluorescence quantum yields and lifetimes

Fluorescence quantum yields (Φ_F) were determined by the comparative method using equation 1.⁴⁻⁵

$$\Phi_F = \frac{F \times A_{std} \times \eta^2}{F_{std} \times A \times \eta_{std}^2} \quad \text{eq. (1)}$$

where F and F^{std} are the areas under the fluorescence emission curves of the samples (**6a-9b**) and the standard (Unsubstituted **ZnPc**), respectively. A and A^{std} are the relative absorbance of the samples and standard at the excitation wavelength, respectively. η^2 and η_{std}^2 are the refractive indices of solvents for the sample and standard, respectively.

Unsubstituted **ZnPc** (in DMF) ($\Phi_F = 0.170$)⁶ was employed as the standard. Both the sample and standard were excited at the same wavelength. The absorbance of the solutions was ranged between 0.10 and 0.12 at the excitation wavelength.

Fluorescence lifetimes τ_F were measured using a time correlated single photon counting setup (TCSPC). The natural radiative lifetimes (τ_0) were evaluated using equation 2.⁷

$$\tau_0 = \frac{\tau_F}{\Phi_F} \quad \text{eq. (2)}$$

1.4. Photochemical Parameters

1.4.1. Singlet oxygen quantum yields

Singlet oxygen quantum yield (Φ_Δ) determinations were carried out using the experimental set-up described in literature.⁸⁻¹¹ Typically, a 3 mL portion of the respective unsubstituted, peripherally, non-peripherally tetra-substituted and octa-substituted Zn(II) Pc and In(III) ClPc solutions (concentration = 1×10^{-5} M) containing the singlet oxygen quencher was irradiated in the Q band region with the photo-irradiation set-up described in the reference.⁸⁻¹¹ Φ_Δ values were determined in air using the relative method with unsubstituted **ZnPc** (in DMF) as references. Diphenylisobenzofurane (DPBF) was used as chemical quencher for singlet oxygen in DMF. The Φ_Δ values of the studied Pc complexes were calculated using equation 3:

$$\Phi_\Delta = \Phi_\Delta^{std} \frac{R \times I_{abs}^{std}}{R^{std} \times I_{abs}} \quad \text{eq. (3)}$$

where Φ_Δ^{std} is the singlet oxygen quantum yield for the standard. Unsubstituted **ZnPc** ($\Phi_\Delta^{std} = 0.56$ in DMF)¹² was used as standard. R and R^{std} are the DPBF photobleaching rates in the presence of the respective samples (**6a-9b** and Unsubs. **ZnPc**) and standard, respectively. I_{abs} and I_{abs}^{std} are the rates of light absorption by the samples and standards, respectively. I_{abs} was determined by using equation 4.

$$I_{abs} = \frac{\alpha \times S \times I}{N_A} \quad \text{eq. (4)}$$

N_A is the Avogadro's constant, S is the irradiated cell area, α is the irradiation time and I_{abs} is the overlap integral of the radiation source light intensity and the absorption of the samples (**6a-9b** and Unsubs. **ZnPc**).

To avoid chain reactions induced by DPBF in the presence of singlet oxygen, the concentration of quenchers (DPBF) was lowered to $\sim 3 \times 10^{-5}$ M.⁸⁻¹¹ Solutions of sensitizer (concentration = 1×10^{-5}) containing DPBF were prepared in the dark and irradiated in the Q band region using the setup described in literature.⁸⁻¹¹ DPBF degradation at 417 nm was monitored. The light intensity used for Φ_Δ determinations was found to be 6.60×10^{15} photons $s^{-1} cm^{-2}$.

1.4.2. Photodegradation quantum yields

Photodegradation quantum yield (Φ_d) determinations were carried out using the experimental set-up described in literature [12]. Photodegradation quantum yields were determined using equation 5,

$$\Phi_d = \frac{(C_0 - C_t) \times V \times N_A}{I_{abs} \times S \times t} \quad \text{eq. (5)}$$

where C_0 and C_t are the samples (Unsubs. **ZnPc**, **6a-9b**) concentrations before and after irradiation respectively, V is the reaction volume, N_A is the Avogadro's constant, S is the irradiated cell area, t is the irradiation time and I_{abs} is the overlap integral of the radiation source

light intensity and the absorption of the samples (**6a-9b** and Unsubs. **ZnPc**). A light intensity of 2.15×10^{16} photons $s^{-1} cm^{-2}$ was employed for Φ_d determinations.

1.4.3. Fluorescence quenching by benzoquinone or potassium iodide (BQ or KI)

Fluorescence quenching experiments on the substituted ZnPc (**6a-9a**) were carried out by the addition of different concentrations of quencher [BQ] or [KI] to a fixed concentration of the complexes, and the concentrations of quencher in the resulting mixtures were 0, 0.008, 0.016, 0.024, 0.032 and 0.040 M. The fluorescence spectra of substituted ZnPc (**6a-9a**) at each quencher concentration were recorded, and the changes in fluorescence intensity related to quencher concentration by the Stern–Volmer equation¹² (equation 6):

$$\frac{I_0}{I} = 1 + K_{sv}[\text{Quencher concentration}] \quad \text{eq. (6)}$$

where I_0 and I are the fluorescence intensities of fluorophore in the absence and presence of quencher, respectively, [BQ] or [KI] is the concentration of the quencher, and K_{sv} is the Stern–Volmer constant, and is the product of the bimolecular quenching constant (k_q) and the fluorescence lifetime τ_F , i.e.

$$K_{sv} = k_q \times \tau_F \quad \text{eq. (7)}$$

The ratios I_0/I were calculated and plotted against [BQ] or [KI] according to equation 6, and K_{sv} determined from the slope.

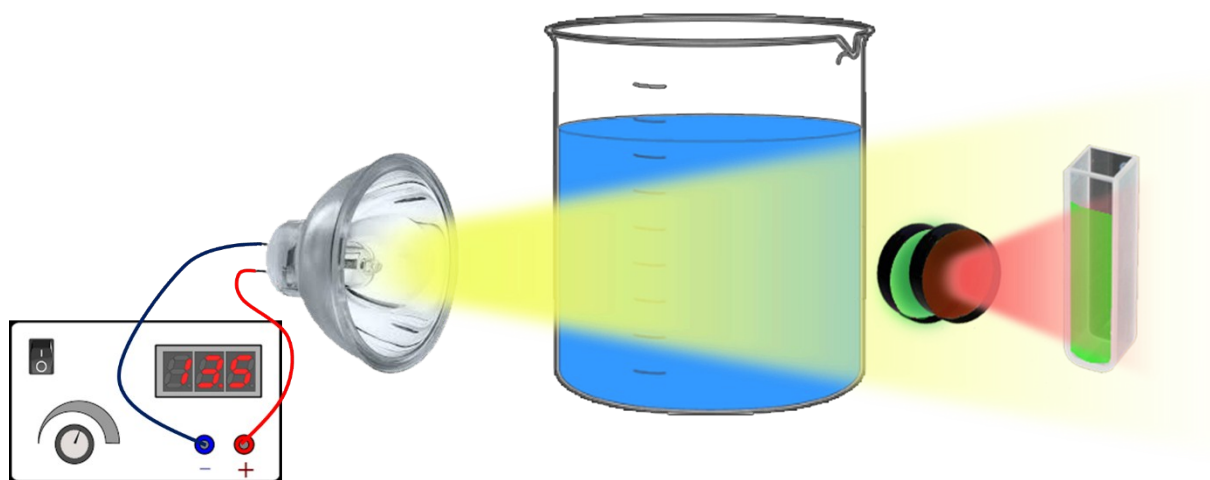


Fig. S1. Photophysical and photochemical measurement process.

2. References

- 1 H. Kuruca, B. Köksoy, B. Karapınar, M. Durmuş and M. Bulut, *J. Porphyr. Phthalocyanines*, 2018, **22**, 266–278.
- 2 O. S. Can, A. Kuş, E. N. Kaya, M. Durmuş and M. Bulut, *Inorganica Chim. Acta*, 2017, **465**, 31–37.
- 3 M. A. Köksoy, B. Köksoy, M. Durmuş and M. Bulut, *J. Organomet. Chem.*, 2016, **822**, 125–134.
- 4 G. İlke, M. Durmuş, V. Ahsen and T. Nyokong, *Dalton Trans.*, 2007, **0**, 3782-3791.
- 5 S. Fery-Forgues and D. Lavabre, *J. Chem. Educ.*, 1999, **76**, 1260-1264.
- 6 A. Ogunsipe, D. Maree and T. Nyokong, *J. Mol. Struct.*, 2003, **650**, 131–140.
- 7 G. Dilber, H. Altunparmak, A. Nas, H. Kantekin and M. Durmuş, *Spectrochim. Acta A.*, 2019, **217**, 128-140.
- 8 B. Ghazal, A. Husain, A. Ganesan, M. Durmuş, X. F. Zhang and S. Makhseed, *Dyes Pigm.*, 2019, **164**, 296-304.
- 9 T. Nyokong and E. Antunes, in *Handbook of Porphyrin Science*, Eds. K. M. Kadish, K. M. Smith and R. Guilard, World Scientific, New York, 2010, pp.247-357.
- 10 Y. Zorlu, F. Dumoulin, M. Durmuş and V. Ahsen, *Tetrahedron*, 2010, **66**, 3248–3258.
- 11 W. Spiller, H. Kliesch, D. Wöhrle, S. Hackbarth, B. Roder and G. Schnurpfeil, *J. Porphyr. Phthalocyanines*, 1998, **2**, 145–158.
- 12 A. Awaji, B. Köksoy, M. Durmuş, A. Aljuhani and S. Alraqa, *Molecules*, 2018, **24**, 77.

Table S1. The specific IR bands of the compounds (1-5, 6a-9b and unsub. ZnPc, InPc)

The Compounds	Aromatic -O-H	Aromatic -C-H	Aliphatic -C-H	-C≡N	Lactone -C=O	Aromatic -C=C-	Ar-O-Ar
1	3203	3062	2925 2854	-	1701	1573	-
2	-	3049	2929 2860	2234	1696	1592	1275
3	-	3087	2923 2856	2234	1703	1569	1277
4	-	3047	2926 2855	2233	1703	1573	1256
5	-	3049	2926 2855	2230	1705	1574	1257
6a	-	3064	2924 2852	-	1707	1569	1211
7a	-	3065	2924 2852	-	1709	1571	1215
8a	-	3067	2926 2854	-	1707	1572	1257
9a	-	3075	2925 2855	-	1705	1571	1257
Unsubs. ZnPc	-	3069	2922 2863	-	1711	1569	-
6b	-	3065	2924 2852	-	1709	1571	1215
7b	-	3072	2923 2853	-	1706	1569	1238
8b	-	3065	2925 2856	-	1707	1571	1256
9b	-	3062	2925 2854	-	1705	1572	1255
Unsubs. InPc	-	3058	2926 2860	-	1722	1548	-

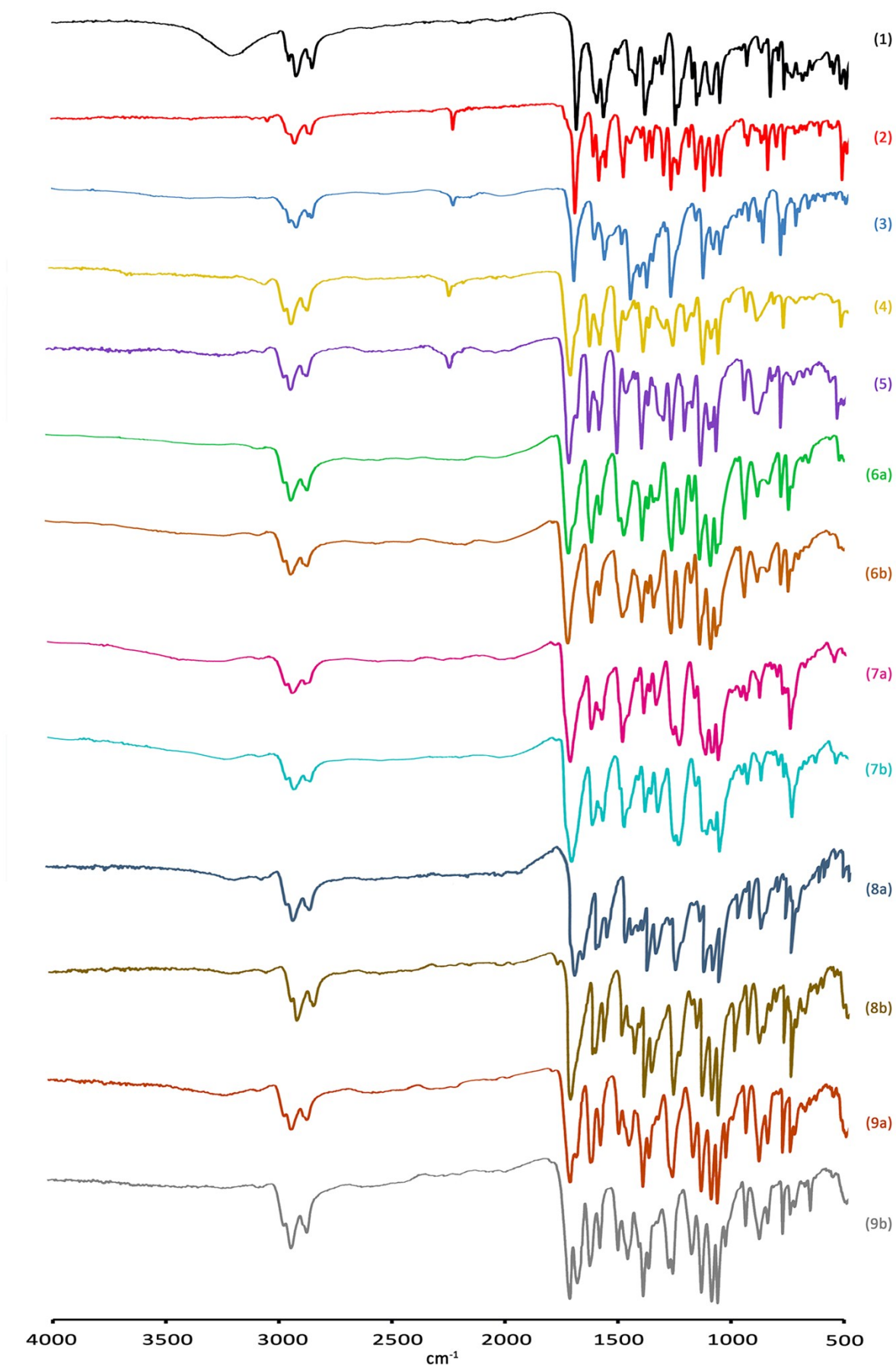
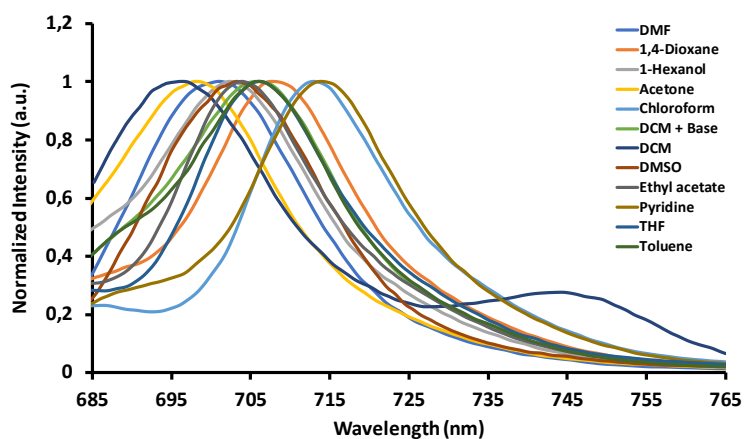


Fig. S2. The IR spectra of the compounds (1-5, 6a-9a, 6b-9b).

Table S2. Absorption and emission spectral results of **7a** in different solvents.

Solvent	$\lambda_{max}^{Q \text{ band}}$ (log ϵ)	$\lambda_{max}^{B \text{ band}}$ (log ϵ)	$\lambda_{max}^{Shoulder}$ (log ϵ)	$\lambda_{max}^{J \text{ Aggregation}}$ (log ϵ)	λ_{max}^{em} (nm)	$\Delta\nu$ (cm^{-1})
Dichloromethane	697 (5.04)	330 (4.99)	629 (4.28)	745 (4.37)	696	21
Dichloromethane + K_2CO_3	693 (5.08)	325 (4.95)	624 (4.34)	-	706	266
Chloroform	697 (4.83)	325 (5.15)	645 (4.42)	741 (5.07)	713	322
Chloroform + K_2CO_3	693 (5.03)	326 (4.88)	624 (4.26)	-	713	405
Acetone	688 (5.06)	324 (4.87)	620 (4.28)	-	698	208
Dimethylformamide	691 (5.11)	325 (4.96)	623 (4.33)	-	700	186
Pyridine	693 (5.11)	324 (5.00)	623 (4.34)	-	714	424
Dimethylsulfoxide	697 (5.11)	324 (4.99)	627 (4.34)	-	703	122
Ethyl acetate	688 (5.09)	322 (4.97)	621 (4.31)	-	704	330
Toluene	694 (5.11)	321 (4.98)	625 (4.32)	-	706	245
Tetrahydrofuran	689 (5.10)	323 (4.94)	621 (4.32)	-	706	349
1,4-Dioxane	692 (5.07)	322 (4.93)	623 (4.30)	-	707	307
1-Hexanol	689 (5.10)	325 (4.97)	621 (4.31)	-	702	269

**Fig. S3.** Emission spectra of compound **7a** in different solvents.

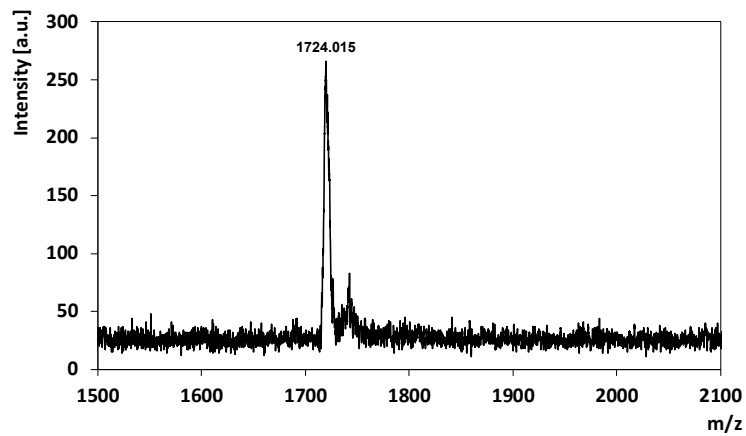


Fig. S4. Positive ion in reflectron mode MALDI-TOF mass spectrum of compound **7a** were obtained in dithranol (DIT).

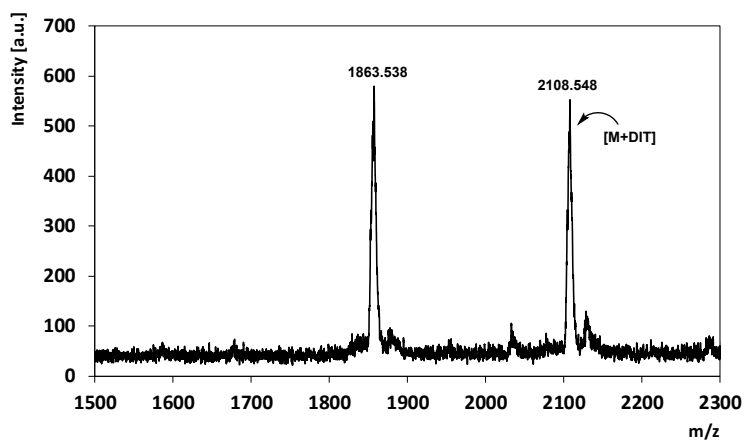


Fig. S5. Positive ion in reflectron mode MALDI-TOF mass spectrum of compound **8a** were obtained in dithranol (DIT).

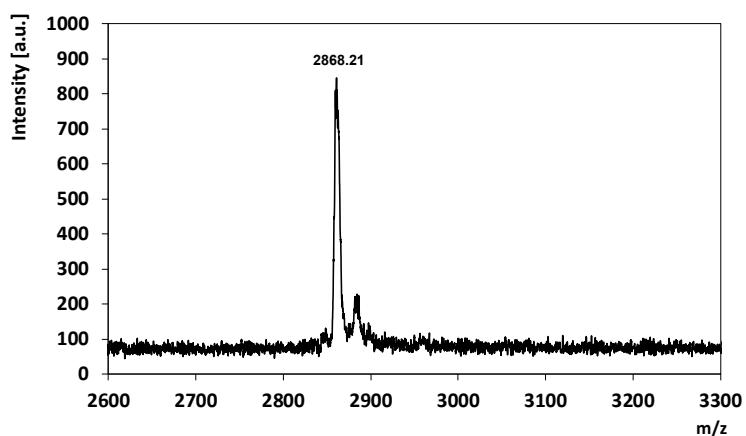


Fig. S6. Positive ion in reflectron mode MALDI-TOF mass spectrum of compound **9a** were obtained in dithranol (DIT).

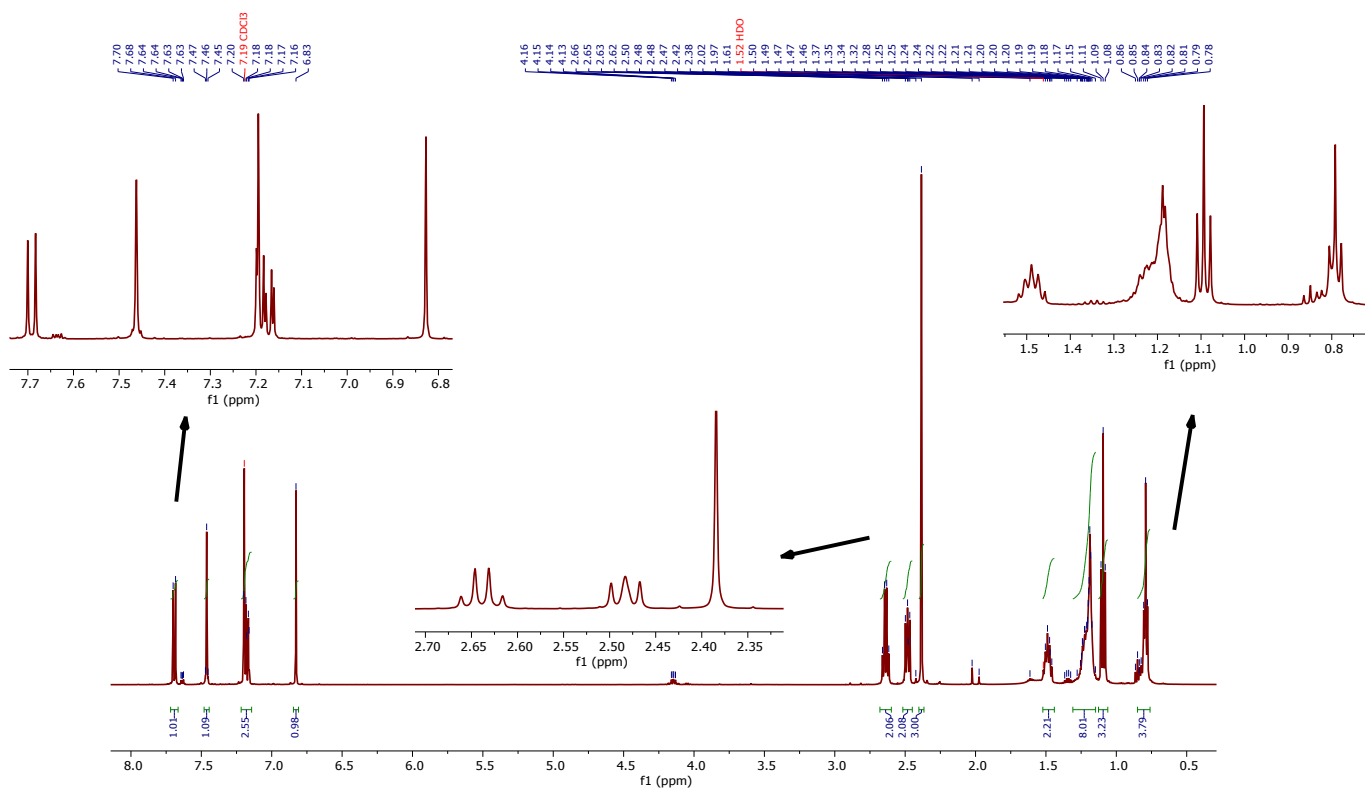
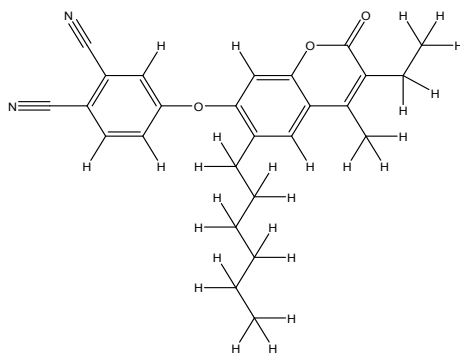


Fig. S8. ^1H NMR spectrum of compound 2.

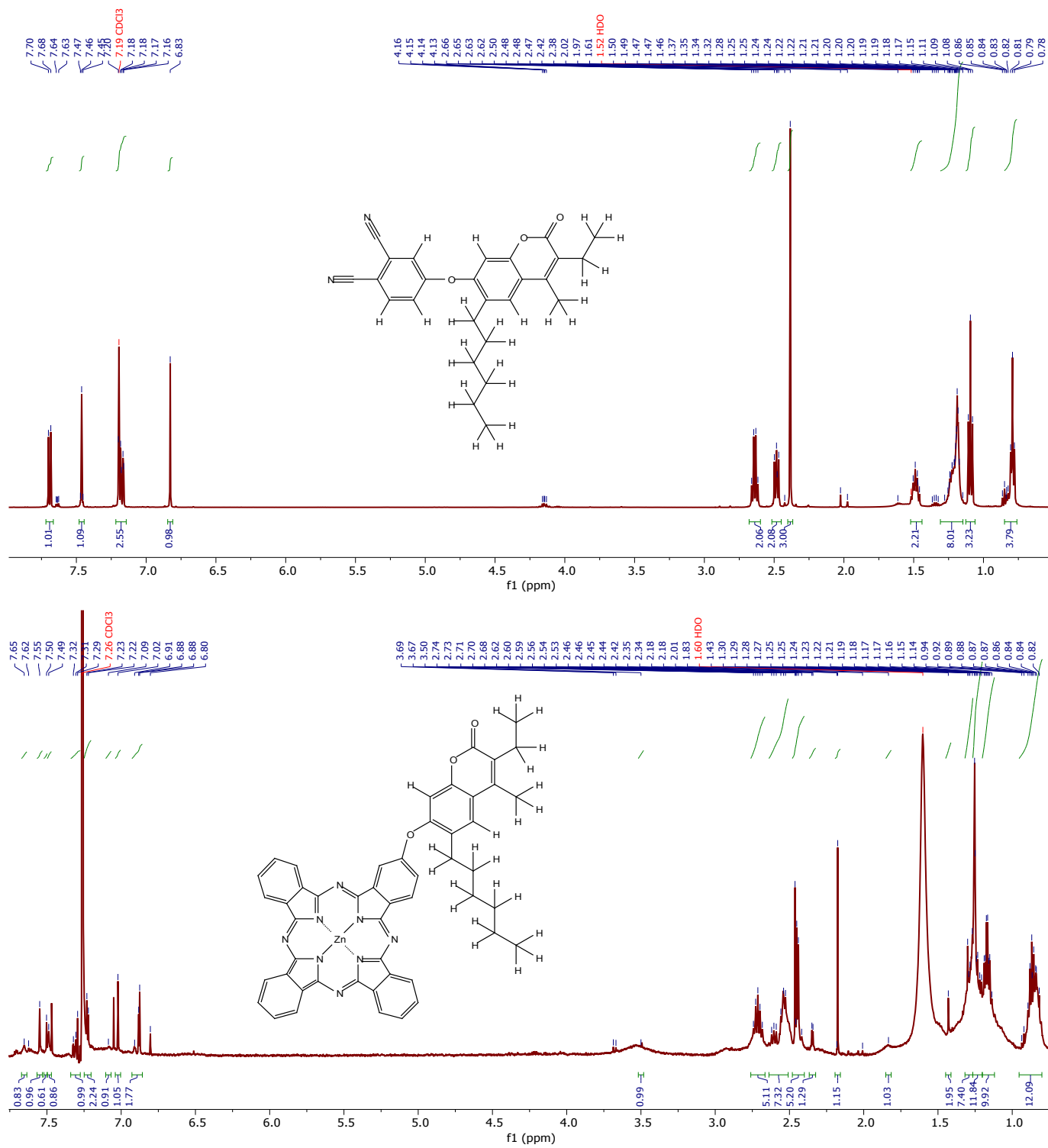


Fig. S9. ^1H NMR spectrum of compound 6a.

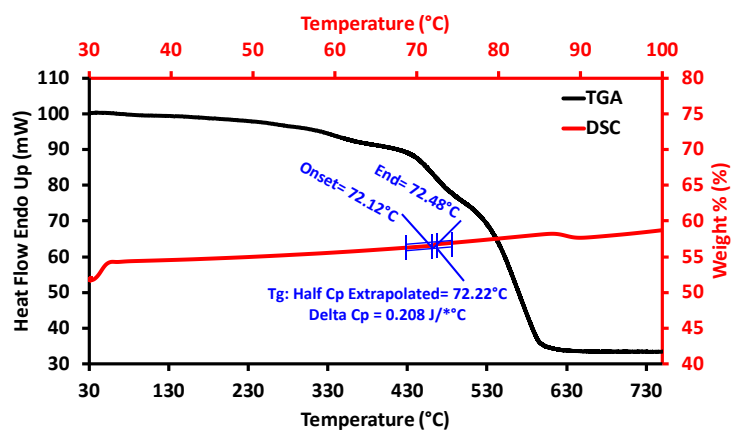


Fig. S10. TGA and DSC curves of compound **6b**.

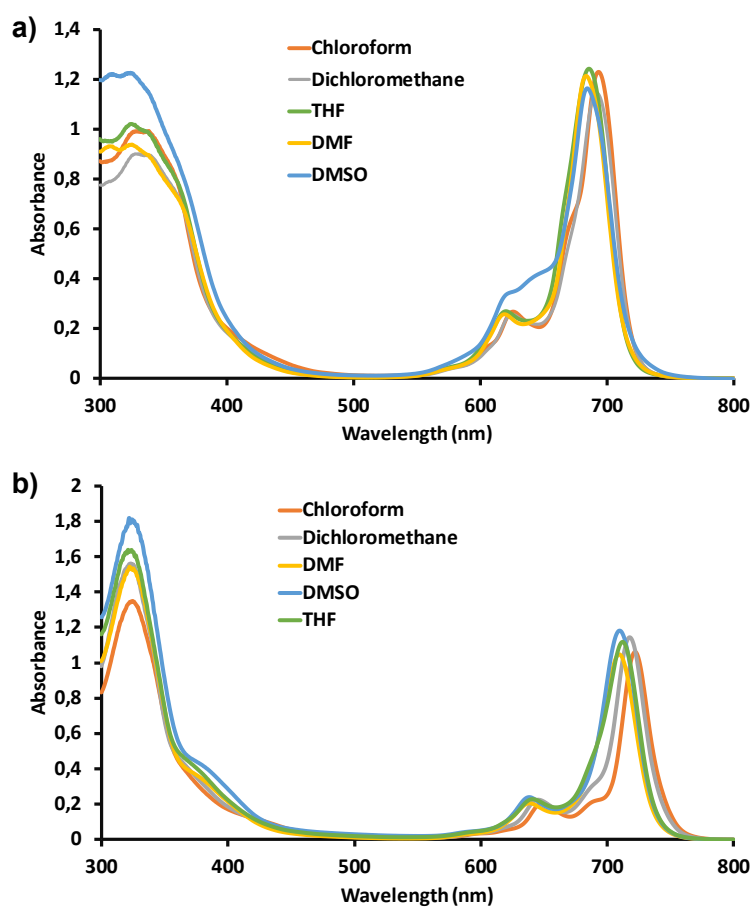


Fig. S11. a) UV-vis spectrums of **6b** in different solvents. b) UV-vis spectrums of **7b** in different solvents.

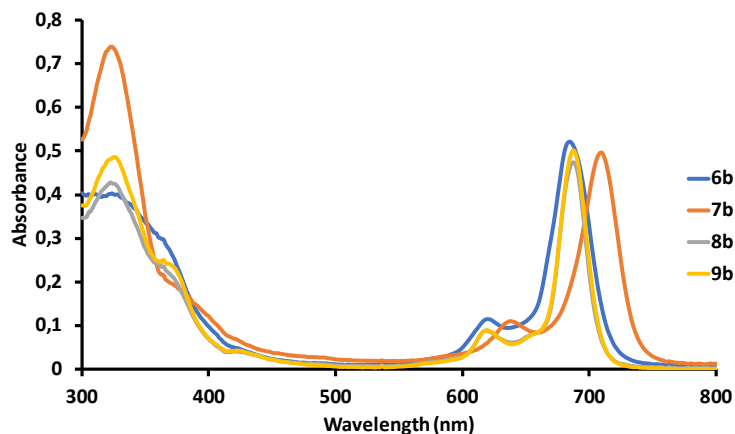


Fig. S12. Absorption spectra of indium phthalocyanine complexes (**6b-9b**) in DMF.

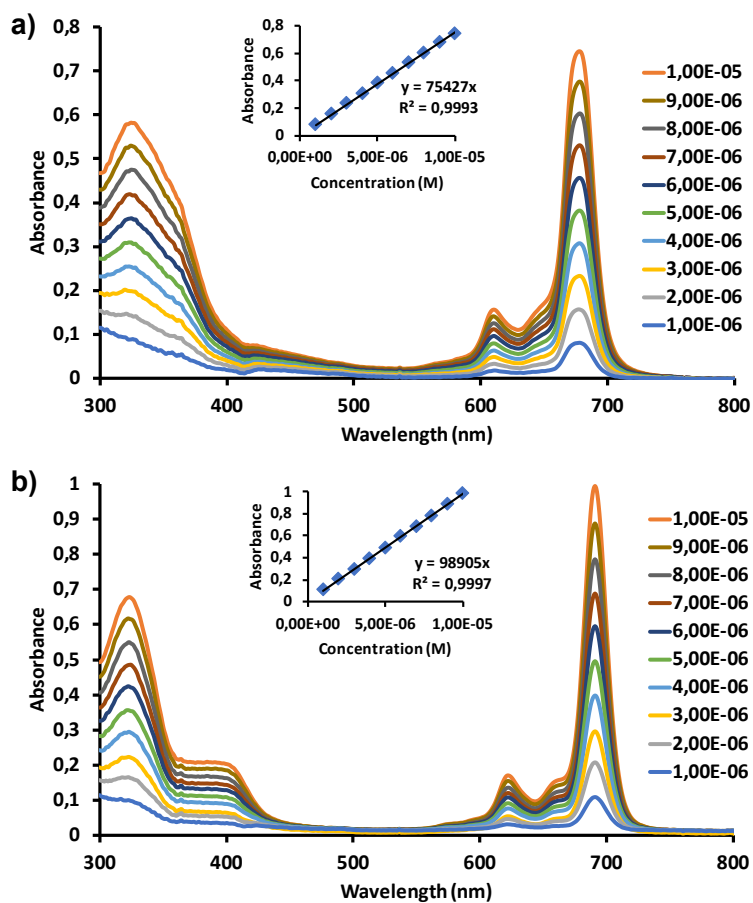


Fig. S13. a) Aggregation behaviors of **8b** in DMF at different concentrations. b) Aggregation behaviors of **7a** in DMF at different concentrations.

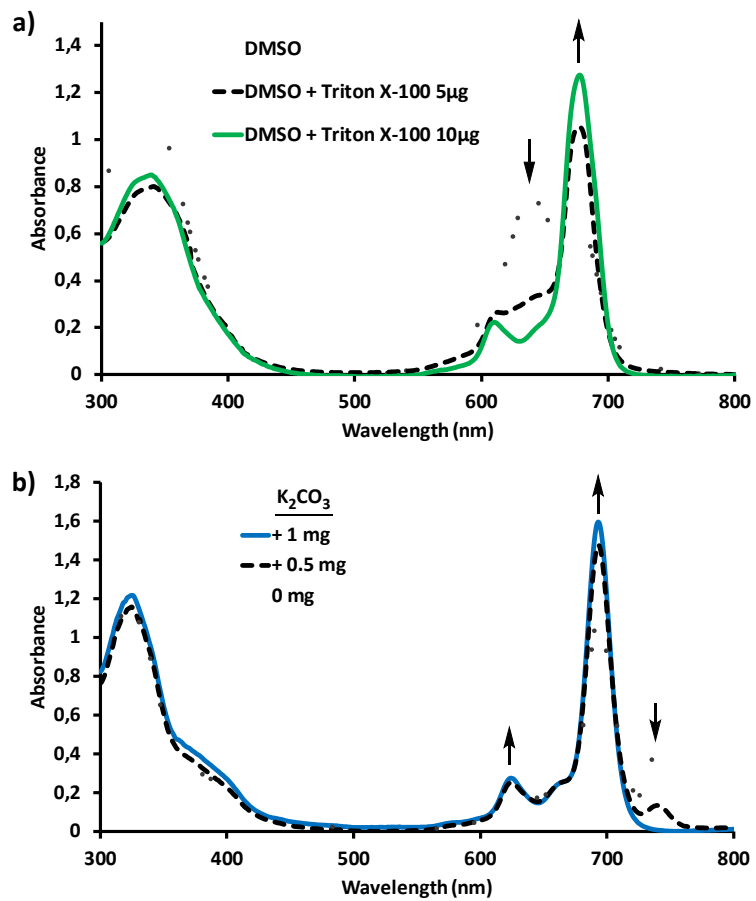


Fig. S14. a) Absorption spectra of **6a** in DMSO and Triton X-100. Concentration $\sim 1 \times 10^{-5}$ M. b) Absorption spectra of **7a** in dichloromethane and $K_2CO_3 + CH_2Cl_2$ solution. Concentration $\sim 1 \times 10^{-5}$ M.

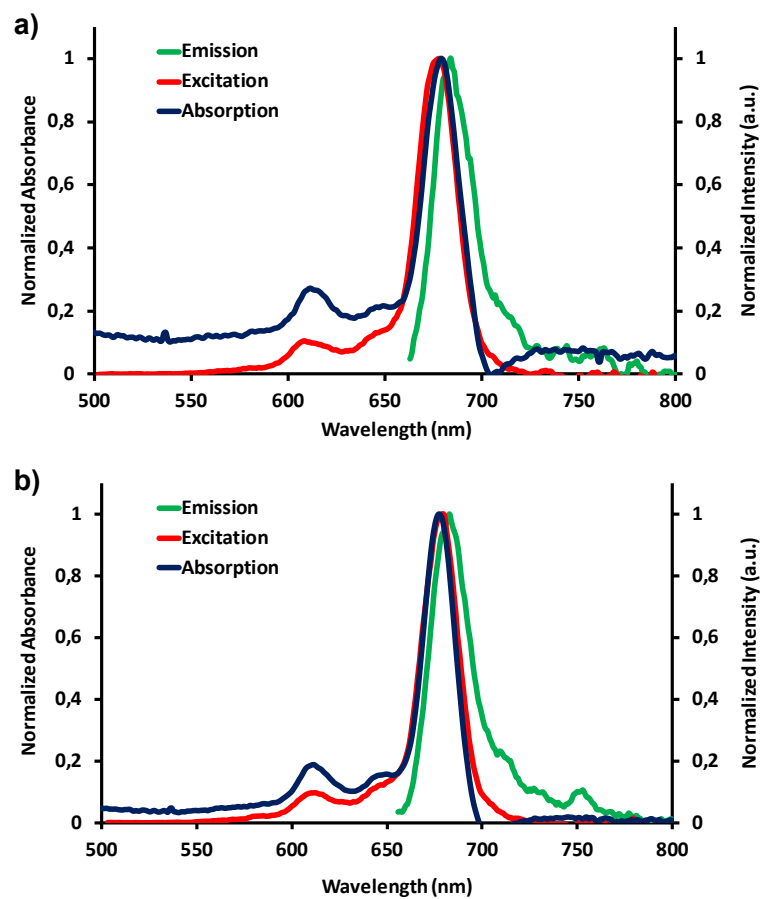


Fig. S15. a) Normalized absorption, emission and excitation spectra for compounds **8a** in DMF. b) Normalized absorption, emission and excitation spectra for compounds **9a** in DMF.

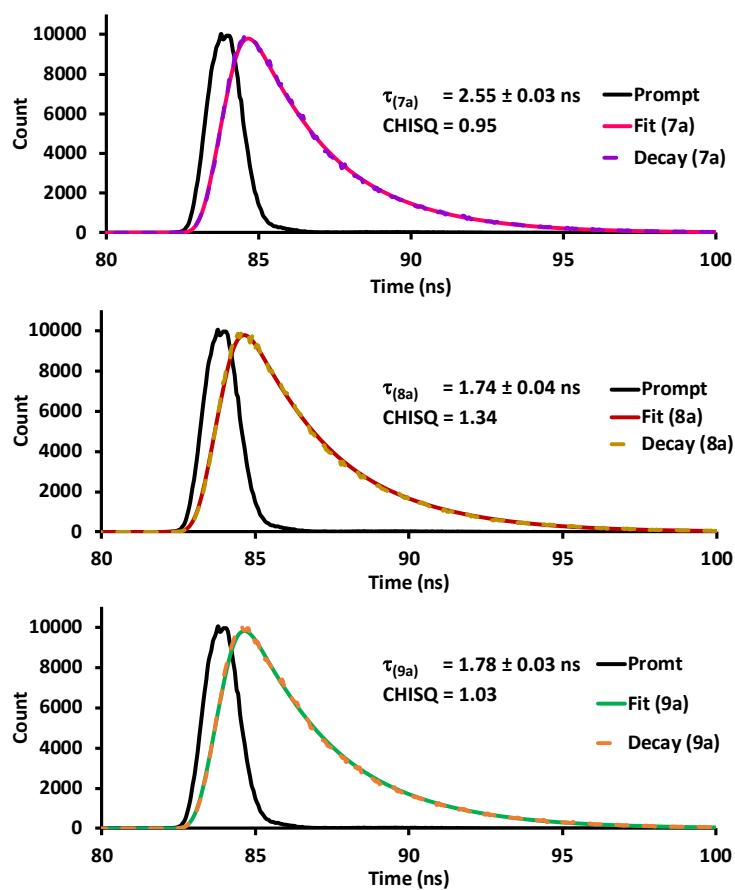


Fig. S16. Time correlated single photon counting (TCSPC) trace for compound **7a**, **8a** and **9a** in DMF with residuals. $\lambda_{\text{EX}} = 661$ nm for **7a**, $\lambda_{\text{EX}} = 650$ nm for **8a** and $\lambda_{\text{EX}} = 644$ nm for **9a**.

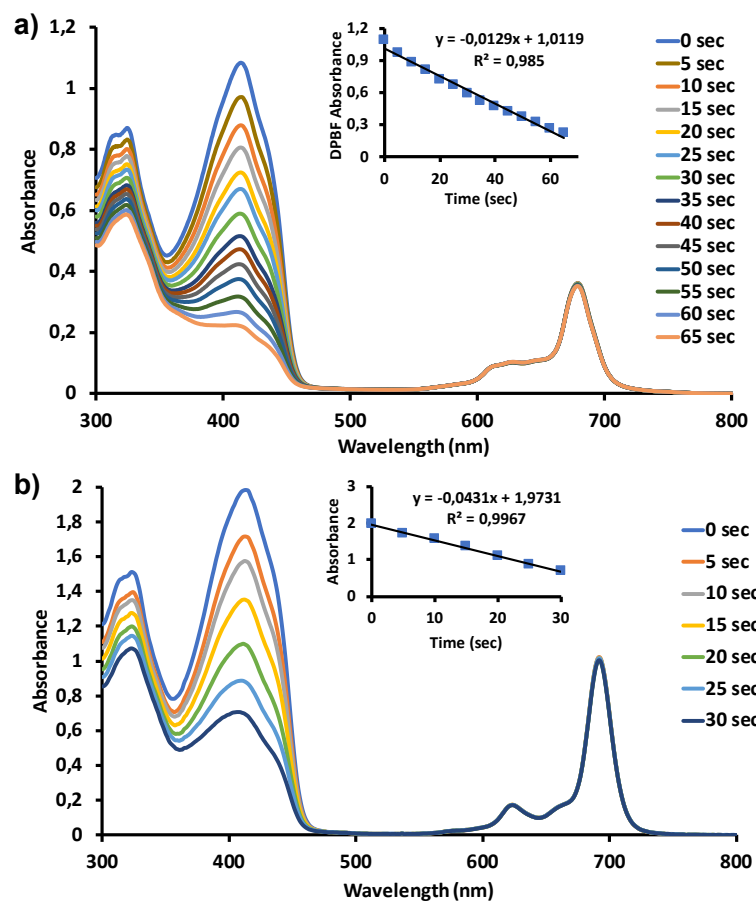


Fig. S17. a) A typical spectra for the determination of singlet oxygen quantum yield of **8a**, in DMF at 1×10^{-5} M (inset: plots of DPBF absorbance versus time). b) A typical spectra for the determination of singlet oxygen quantum yield of **9b**, in DMF at 1×10^{-5} M (inset: plots of DPBF absorbance versus time).

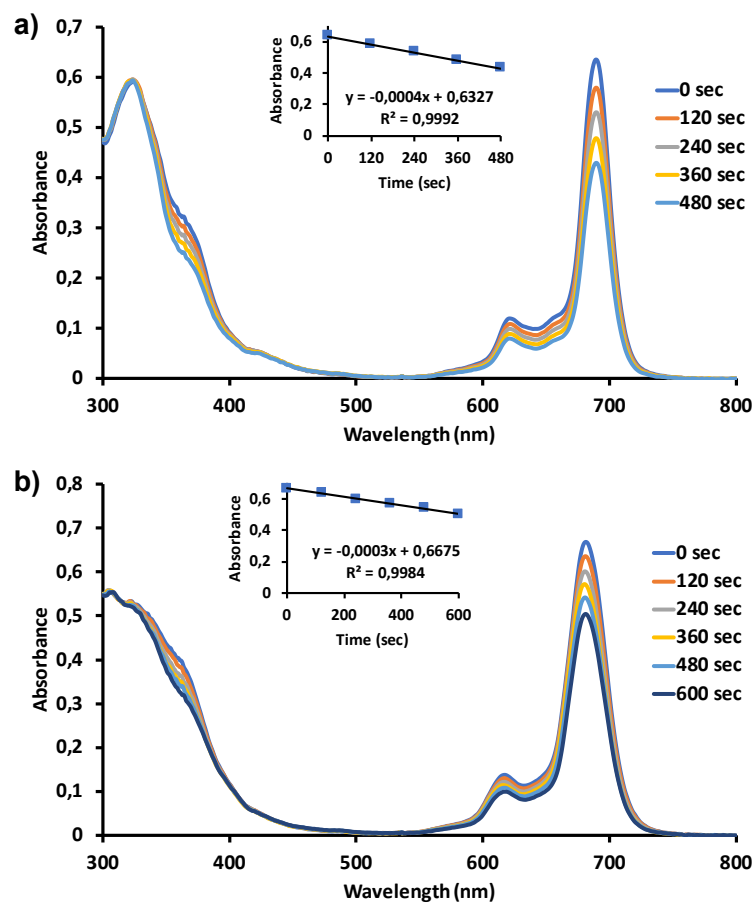


Fig. S18. a) The photodegradation of compounds **8b** in DMF showing the disappearance of the Q-band at eight minutes intervals. b) The photodegradation of compounds **6b** in DMF showing the disappearance of the Q-band at ten minutes intervals.

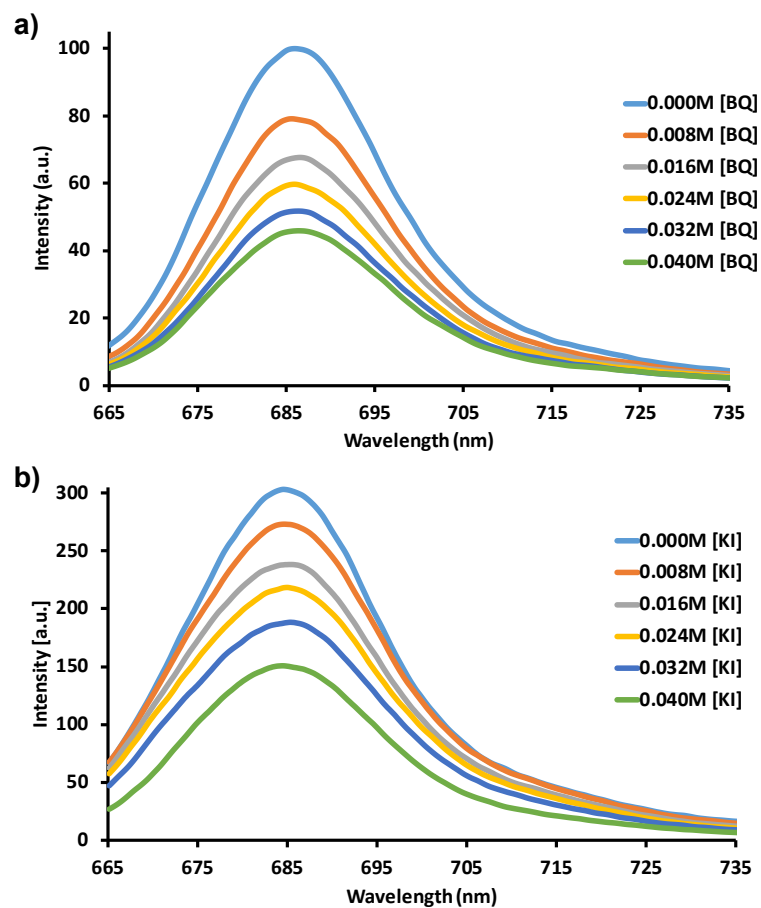


Fig. S19. a) Fluorescence emission spectral changes of compound **8a** on addition of different concentrations of BQ in DMF. b) Fluorescence emission spectral changes of compound **9a** on addition of different concentrations of KI in DMF. Concentration $\sim 1 \times 10^{-6}$ M.

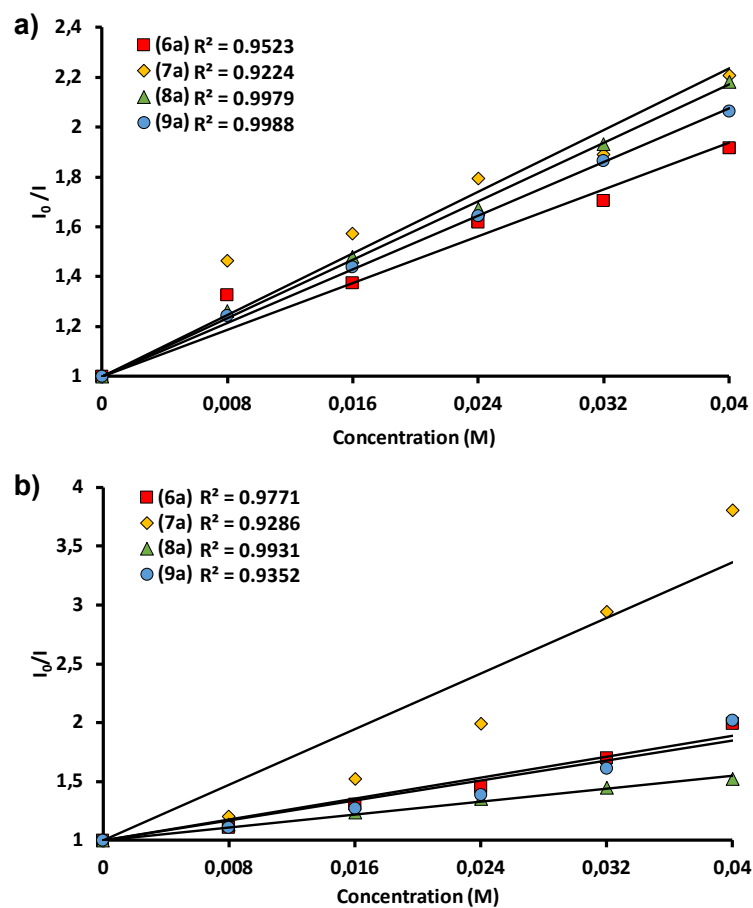


Fig. S20 a) Stern-Volmer plots for 1,4-benzoquinone (BQ) quenching of **6a**, **7a**, **8a** and **9a**, concentration: $\sim 1 \times 10^{-6}$ M in DMF. b) Stern-Volmer plots for potassium iodide (KI) quenching of **6a**, **7a**, **8a** and **9a**, concentration: $\sim 1 \times 10^{-6}$ M in DMF. [BQ] and [KI] concentration = 0, 0.008, 0.016, 0.024, 0.032, 0.040 M.